Hole-doping dependence of the magnetic penetration depth and vortex core size in $YBa_2Cu_3O_y$: Evidence for stripe correlations near $\frac{1}{8}$ hole doping

J. E. Sonier,[1,2] S. A. Sabok-Sayr,[1] F. D. Callaghan,[1] C. V. Kaiser,[1] V. Pacradouni,[1] J. H. Brewer,[2,3] S. L. Stubbs,[3] W. N. Hardy,[2,3] D. A. Bonn,[2,3] R. Liang,[2,3] and W. A. Atkinson[4]

[1]*Department of Physics, Simon Fraser University, Burnaby, British Columbia, Canada V5A 1S6*

[2]*Canadian Institute for Advanced Research, 180 Dundas Street West, Toronto, Ontario, Canada M5G 1Z8*

[3]*Department of Physics and Astronomy, University of British Columbia, Vancouver, British Columbia, Canada V6T 1Z1*

[4]*Department of Physics and Astronomy, Trent University, Peterborough, Ontario, Canada K9J 7B8*

(Received 20 June 2007; published 31 October 2007)

We report on muon spin rotation measurements of the internal magnetic field distribution $n(B)$ in the vortex solid phase of $YBa_2Cu_3O_y$ (YBCO) single crystals, from which we have simultaneously determined the hole-doping dependences of the in-plane Ginzburg-Landau (GL) length scales in the underdoped regime. We find that T_c has a sublinear dependence on $1/\lambda_{ab}^2$, where λ_{ab} is the in-plane magnetic penetration depth in the extrapolated limits $T\rightarrow 0$ and $H\rightarrow 0$. The power coefficient of the sublinear dependence is close to that determined in severely underdoped YBCO thin films, indicating that the same relationship between T_c and the superfluid density is maintained throughout the underdoped regime. The GL coherence length ξ_{ab} (vortex core size) is found to increase with decreasing hole-doping concentration and to exhibit a field dependence that is explained by proximity-induced superconductivity on the CuO chains. Both λ_{ab} and ξ_{ab} are enhanced near $\frac{1}{8}$ hole doping, supporting the belief by some that stripe correlations are a universal property of high-T_c cuprates.

DOI: 10.1103/PhysRevB.76.134518 PACS number(s): 74.25.Qt, 74.72.Bk, 76.75.+i

I. INTRODUCTION

Abrikosov vortices in a superconductor are governed by two characteristic length scales. The core of a vortex has a size dependent on the Ginzburg-Landau (GL) coherence length ξ, while the supercurrents circulating around the core decay on the scale of the GL penetration depth λ. In the early days of high-T_c superconductivity, it was common practice to infer the behavior of the in-plane magnetic penetration depth λ_{ab} from measurements of the muon depolarization rate σ in the vortex state of polycrystalline samples. The temperature dependence of σ was found to be consistent with *s*-wave pairing symmetry[1–4] and a universal linear scaling of T_c with σ was observed in the underdoped regime (the so-called "Uemura plot"), indicating that $T_c\propto 1/\lambda_{ab}^2\propto\rho_s$, where ρ_s is the superfluid density.[5,6] Later, microwave[7] and muon spin rotation (μSR)[8] measurements on $YBa_2Cu_3O_y$ (YBCO) single crystals in the Meissner and vortex phases established a limiting low-temperature linear T dependence of λ_{ab} that is consistent with *d*-wave pairing. More recently, non-μSR studies of YBCO in the Meissner phase have revealed that T_c has a sublinear dependence on $1/\lambda_{ab}^2$.[9–11] On the other hand, the relation $T_c\propto\rho_s$ inferred from the Uemura plot is supported by a recent study of electric-field-induced superfluid density modulations in a single underdoped ultrathin film of $La_{2-x}Sr_xCuO_4$.[12]

The problem with assuming $\sigma\propto 1/\lambda_{ab}^2$ is that there are additional inseparable contributions to σ from electronic magnetic moments and flux-line lattice (FLL) disorder, which may vary with doping. To circumvent this difficulty, we have studied YBCO single crystals. In a single crystal, the FLL contribution to the μSR line shape $n(B)$ is asymmetric and distinct from the other sources of field inhomogeneity.[13] Not only can the behavior of λ_{ab} be isolated, but because the finite size of the vortex cores is apparent in a single-crystal measurement of $n(B)$, ξ_{ab} can be simultaneously determined. While ξ_{ab} may be accurately determined in conventional superconductors from measurements of the upper critical field H_{c2}, in high-T_c cuprates H_{c2} is generally a very high magnetic field marking the transition from a vortex liquid to the normal phase. Here, we present μSR measurements that probe λ_{ab} and ξ_{ab} in the bulk of YBCO single crystals deep in the superconducting state. The accuracy of our method was demonstrated in previous studies of conventional superconductors,[14–16] but is reinforced here through comparisons with the results from other techniques.

II. EXPERIMENTAL DETAILS

YBCO single crystals with purity of 99.995% were grown by a self-flux method in fabricated $BaZrO_3$ crucibles at the University of British Columbia.[17] An exception are $y=6.60$ single crystals that were grown in yttria-stabilized-zirconia crucibles and characterized by a purity greater than 99.5%.[18] Single crystals of Ca-doped YBCO were also prepared in $BaZrO_3$ crucibles. Typical sample sizes consisted of three to five single crystals from the same growth batch arranged in a mosaic to form a total $\hat{a}$-$\hat{b}$ surface area of 20–30 mm^2. The thicknesses of the crystals are on the order of $\sim$0.1 mm. The superconducting transition temperatures of the single crystals were measured using a superconducting quantum interference device magnetometer. Twin boundaries were removed from some of the higher-doped single crystals by applying pressure along the $\hat{a}$ or $\hat{b}$ directions at elevated temperature. These basic sample characteristics are summarized in Table I.

The μSR experiments were performed over a 3 year period on the M15 and M20B surface muon beam lines at

TABLE I. Characteristics of the $YBa_2Cu_3O_y$ and $(Y,Ca)Ba_2Cu_3O_{6.98}$ single crystals. The hole concentration p per CuO_2 layer is determined from the dependence of T_c on p presented in Ref. 19 for similar YBCO single crystals. A $\surd$ indicates which samples were mechanically detwinned.

y	p	T_c (K)	Detwinned
6.60	0.103	62.5	
6.57	0.110	59.0	
6.67	0.120	66.0	
6.75	0.132	74.6	$\surd$
6.80	0.140	84.5	$\surd$
6.95	0.172	93.2	$\surd$
(Y,Ca)6.98	0.192	86.0	

TRIUMF, Vancouver, Canada. The μSR spectra were recorded in a transverse-field (TF) geometry with the applied magnetic field **H** perpendicular to the initial muon spin polarization direction and parallel to the c axis of the single crystals. A TF-μSR spectrum comprised of $(20-30)\times 10^6$ muon decay events was taken at each temperature and magnetic field.

In a transverse field, the muon spin precesses in a plane perpendicular to the field direction (which we define here as the z direction). The time evolution of the muon spin polarization $P(t)$ is determined from the μSR "asymmetry" spectrum formed from the muon decay events detected in opposing positron counters,

$$A(t) = \frac{N_1(t) - N_2(t)}{N_1(t) + N_2(t)} = a_0 P(t), \tag{1}$$

where $N_1(t) = N_0 e^{-t/\tau_\mu}[1 + a_0 P(t)]$ and $N_2(t) = N_0 e^{-t/\tau_\mu}[1 - a_0 P(t)]$ are the time histograms of the temporal dependence of decay positron count rate in detectors 1 and 2 after subtracting a time-independent background, N_0 is the initial counting rate, τ_μ is the muon lifetime, and a_0 is the asymmetry maximum. In our experiments, four positron counters were used to completely cover the 360° solid angle in the x-y plane (see Fig. 1). The muon spin polarization function for the "Left"-"Right" pair of detectors is defined as

$$P_x(t) = \int_0^\infty n(B)\cos(\gamma_\mu B t + \phi) dB, \tag{2}$$

and for the "Up"-"Down" pair as

$$P_y(t) = \int_0^\infty n(B)\cos(\gamma_\mu B t + \phi - \pi/2) dB, \tag{3}$$

where γ_μ is the muon gyromagnetic ratio, ϕ is a phase constant, and

$$n(B') = \langle \delta[B' - B(\mathbf{r})] \rangle \tag{4}$$

is the probability of finding a local magnetic field B in the z direction at an arbitrary position **r** in the x-y plane.

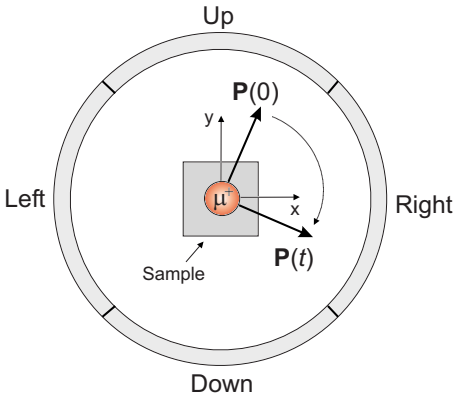

FIG. 1. (Color online) Schematic of the positron counter arrangement used in the present study. The muon beam axis and the applied magnetic field are perpendicular to the page (i.e., parallel to the z axis). The muon spin precesses in the x-y plane about the local z component of the magnetic field before undergoing the decay $\mu^+ \rightarrow e^+ + \nu_e + \bar{\nu}_\mu$. In our study, the muon spin polarization $\mathbf{P}(t)$ is formed from approximately $(20-30)\times 10^6$ muon decay events. The decay events detected in the "Left" and "Right" positron counters form the x component of $\mathbf{P}(t)$, while decay events detected in the "Up" and "Down" positron counters form the y component.

III. DATA ANALYSIS METHOD

The TF-μSR time spectra for each sample were fitted assuming the following analytical solution of the GL equations[20] for the spatial field profile of the ideal FLL:

$$B(\mathbf{r}) = B_0 \sum_{\mathbf{G}} \frac{e^{-i\mathbf{G}\cdot\mathbf{r}} F(G)}{\lambda_{ab}^2 G^2}, \tag{5}$$

where **G** are the reciprocal lattice vectors, B_0 is the average internal magnetic field, $F(G) = uK_1(u)$ is a cutoff function for the **G** sum, $K_1(u)$ is a modified Bessel function, and $u = \sqrt{2}\xi_{ab}G$. The cutoff function $F(G)$ depends on the spatial profile of the superconducting order parameter at the center of the vortex core. Consequently, ξ_{ab} is a measure of the *vortex core size*. The FLL in all samples was assumed to be hexagonal. Neutron scattering experiments on fully doped YBCO[21] indicate that the FLL below $H \approx 40$ kOe is only slightly distorted from hexagonal symmetry due to a/b anisotropy. We find that accounting for this small distortion changes the values of ξ_{ab} and λ_{ab} by less than 5%. Consequently, the FLL was assumed to be hexagonal for all samples studied.

To avoid the difficulty of modeling the contribution of electronic magnetic moments to the μSR line shape, we restricted our study to YBCO crystals free of static or quasistatic spins. For the applied fields considered in this study, this has been determined to be the case for oxygen content $y > 6.50$.[22]

To properly account for disorder of the FLL, the dimensionality of the vortices must be considered. Josephson plasma resonance measurements on $YBa_2Cu_3O_{6.50}$ ortho-II single crystals grown by Dulić *et al.* indicate that the vortices are three-dimensional (3D)-like at low temperatures,[23] while mutual inductance measurements on thin films by Zuev *et al.*

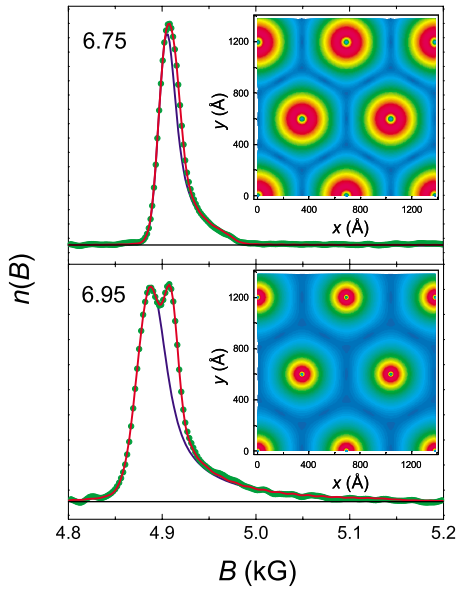

FIG. 2. (Color online) μSR line shapes in single-crystal YBCO. Fourier transforms of the TF-μSR signal from $y=6.75$ and $y=6.95$ samples at $T=2.5$ K and $H=4.92$ kOe (green circles). The right hand peak for $y=6.95$ is a background signal coming from muons stopping outside the sample (note that the background and sample peaks nearly coincide in the μSR line shape for $y=6.75$). The red curves through the data are the Fourier transforms of the fits in the time domain and the blue curves are the sample contribution to the fits (i.e., the difference between the red and blue curves is the contribution from the background signal). The fitted values are $\lambda_{ab}=1796.5$ Å and $\xi_{ab}=44.2$ Å for $y=6.75$, and $\lambda_{ab}=1255.6$ Å and $\xi_{ab}=29.0$ Å for $y=6.95$. The contour plots show the corresponding spatial dependence of the supercurrent density $j(x,y)=|\nabla\times\mathbf{B}(x,y)|$, providing a visual illustration of the change in the core size with hole doping. Note that the core radius corresponds to the center of the light red halo around each vortex.

show that even severely underdoped YBCO is quasi-two-dimensional only near T_c.[10] Since the focus in the present study is on the variation of λ_{ab} and ξ_{ab} in higher-doped samples at low temperatures, the vortices are assumed to be rigid 3D lines of flux. This assumption is also consistent with the observation of highly asymmetric μSR line shapes for all of our samples at low T (see Fig. 2). In particular, the long high-field tail due to the field around the vortex core is a signature of a lattice of rigid 3D flux lines. If on the other hand the vortex lines were highly flexible along their length, the high-field tail would be significantly truncated by random pinning and the line shapes would look more symmetric.[13] As we will see, the reason the high-field tail of the μSR line shape for $YBa_2Cu_3O_{6.75}$ appears shorter than that for $YBa_2Cu_3O_{6.95}$ has to do with both a growth in λ_{ab} and the vortex core size.

For rigid flux lines, random displacements of the vortices from their positions in the ideal hexagonal FLL are accounted for by convoluting the theoretical line shape $n(B)$ by a Gaussian distribution of fields.[24] A Gaussian function also describes the local distribution of dipolar fields originating from static nuclear moments.[25] Taking into account both sources of line broadening, the corresponding theoretical polarization functions are

$$P_x(t) = e^{-\sigma_{\rm eff}^2 t^2/2}\int_0^\infty n(B)\cos(\gamma_\mu Bt+\phi)dB, \tag{6}$$

$$P_y(t) = e^{-\sigma_{\rm eff}^2 t^2/2}\int_0^\infty n(B)\cos(\gamma_\mu Bt+\phi-\pi/2)dB, \tag{7}$$

where

$$\sigma_{\rm eff}^2 = \sigma_{\rm dip}^2 + \sigma_{\rm FLL}^2 \tag{8}$$

is an effective depolarization rate due to nuclear dipole moments ($\sigma_{\rm dip}$) and FLL disorder ($\sigma_{\rm FLL}$). Values for $\sigma_{\rm dip}$ were obtained by fitting the TF-μSR signal above T_c to the theoretical polarization function

$$P(t) = e^{-\sigma_{\rm dip}^2 t^2/2}\cos(\gamma_\mu Bt+\phi). \tag{9}$$

To account for the background signal from muons that did not stop in the sample, an additional term of the form $(1-f)e^{-\sigma_{\rm B}^2 t^2/2}\cos(\gamma_\mu Bt+\phi_{\rm B})$ was added to Eq. (7) and to Eq. (9), where f is the fraction of muons that stopped inside the sample. Values of f for the different samples ranged from 0.8 to 0.9.

In the present work, there are two marked improvements over the analysis done in our previous studies of YBCO single crystals[26–28] that assumed the spatial field profile of Eq. (5): (i) The earlier works used the asymptotic limit $K_1(u)=\sqrt{\pi/2u}\exp(-u)$ $(u\gg 1)$ for the Bessel function that appears in the cutoff $F(\mathbf{G})$, whereas here $K_1(u)$ was evaluated numerically. (ii) The second improvement is that due to increased computer speed, $B(\mathbf{r})$ was calculated at 15 132 equally spaced locations in the rhombic unit cell of the hexagonal FLL, compared to 5628 locations in previous works. Further increasing the number of real-space points sampled in the FLL unit cell did not result in appreciable changes in

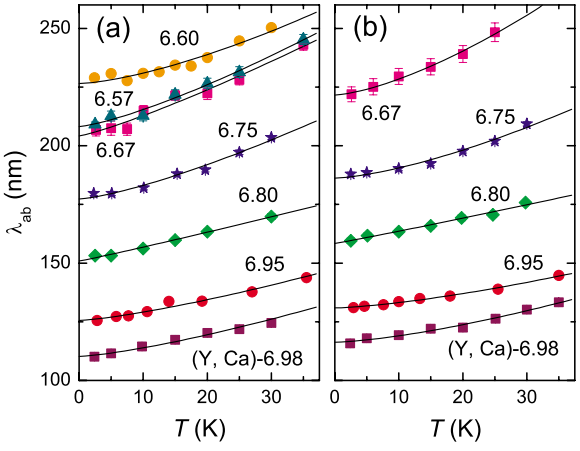

FIG. 3. (Color online) Temperature dependence of λ_{ab} at (a) $H=5$ kOe and (b) $H=15$ kOe. The solid curves are fits to $\lambda_{ab}(T,H)=\lambda_{ab}(0,H)+\alpha T^n$, where α and n are field-dependent coefficients.

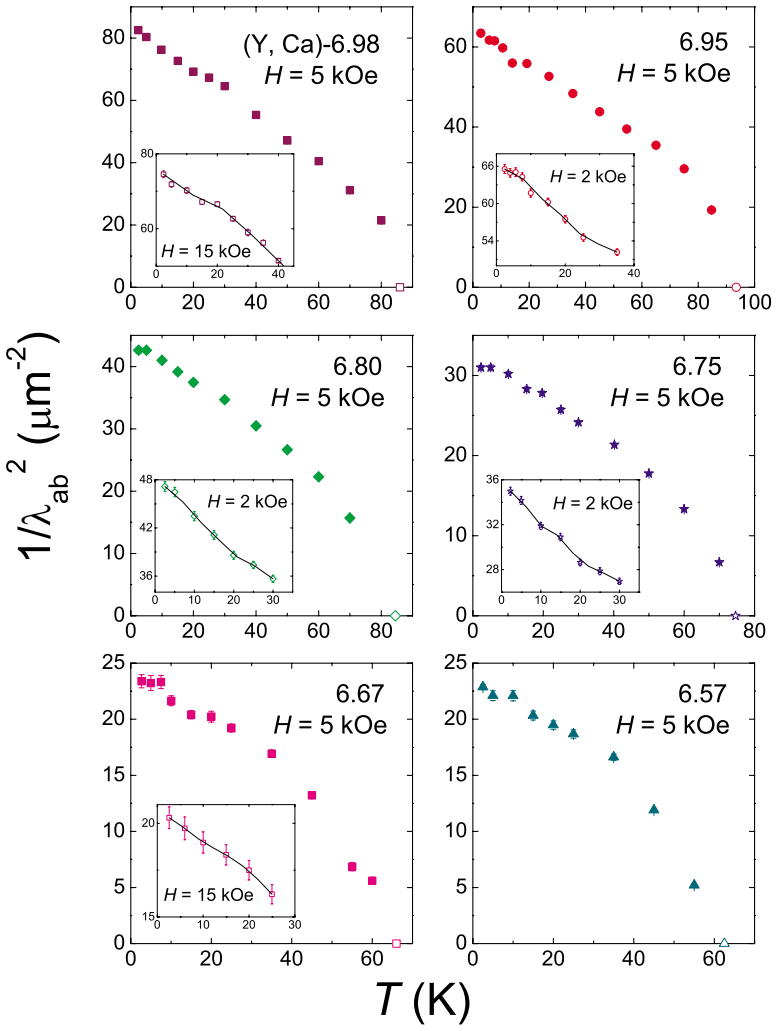

FIG. 4. (Color online) Temperature dependence of $1/\lambda_{ab}^2$ at $H=5$ kOe. The insets show additional low-temperature measurements at $H=2$ kOe or $H=15$ kOe. The solid curves through the data points are merely guides for the eye.

the fitted parameters. We note that both improvements in our data analysis method influence the absolute values of λ_{ab} and ξ_{ab}, but the temperature and magnetic field dependences of these parameters remain qualitatively similar to that determined in our previous studies.

IV. RESULTS FOR λ_{ab}

A. Temperature dependence

Figure 3 shows the temperature dependence of λ_{ab} at low T determined at two different values of the applied magnetic field. The solid curves are fits to $\lambda_{ab}(T,H)=\lambda_{ab}(0,H)+\alpha T^n$, where α and n are field-dependent coefficients. The dependence of $1/\lambda_{ab}^2$ on T is shown in Fig. 4 for selected values of the applied field. An inflection point at $T\approx 20$ K is visible in some of the lower field data. This feature was also apparent in our previous measurements of $YBa_2Cu_3O_{6.95}$.[28] Harshman *et al.* have argued that the inflection point is caused by thermal depinning of vortices,[29] although an invalid treatment of the data was used to support this assertion.[30] Recently, Khasanov *et al.* have ruled out depinning as the source of a similar inflection point in the temperature dependence of $1/\lambda_{ab}^2$ measured in $La_{1.83}Sr_{0.17}CuO_4$ by TF-μSR.[31] Instead, they attribute this feature to the occurrence of both a large d-wave and a small s-wave superconducting gap. As we will show later, the anomalous magnetic field dependence of the vortex core size in YBCO can be explained by an induced superconducting energy gap in the CuO chains that run along the b direction. Theoretical calculations by Atkinson and Carbotte[36] for a d-wave superconductor with proximity-induced superconductivity in the CuO chains show that $1/\lambda_{ab}^2(T)$ exhibits an inflection point caused by an upturn of $1/\lambda_b^2(T)$ at low T (where λ_b is the penetration depth in the b direction).

In Fig. 5, it is shown that $\lambda_{ab}^2(T\rightarrow 0)/\lambda_{ab}^2(T)$ exhibits a near universal linear temperature dependence at low T. We attribute deviations from universal behavior near T_c to softening of the FLL, which narrows the μSR line shape and enhances the fitted value of λ_{ab}. The universal scaling implies that $\lambda_{ab}^2(T\rightarrow 0)T_c v_F Z^{e2}/v_\Delta$ is a constant,[32] where v_F is the Fermi velocity, v_Δ is a velocity corresponding to the slope of the gap at the nodes, and Z^e is a charge renormalization parametrizing the coupling of the quasiparticles to phase fluctuations. Using values of v_Δ from thermal conductivity measurements,[33] we find that Z^e is basically doping independent.

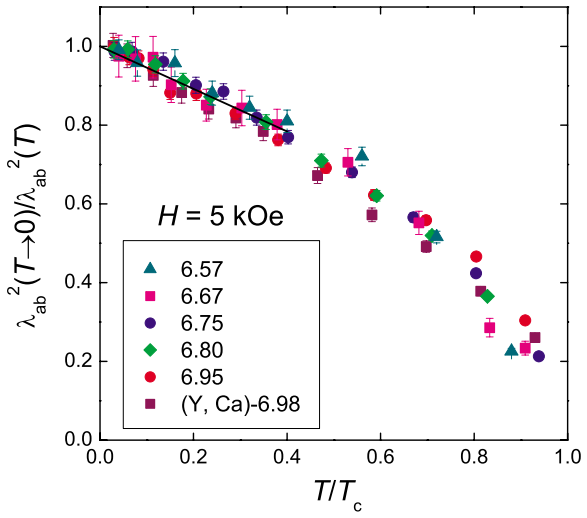

FIG. 5. (Color online) Temperature dependence of $1/\lambda_{ab}^2$ at $H=5$ kOe, normalized to $1/\lambda_{ab}^2(T\rightarrow 0)$ and plotted as a function of reduced temperature T/T_c. The solid line through the data is a fit given by $\lambda_{ab}^2(T\rightarrow 0)/\lambda_{ab}^2(T)=1-0.54T/T_c$.

B. Magnetic field dependence

Figure 6 shows the magnetic field dependences of λ_{ab}. Here, we stress that the observed behaviors do not imply that the magnetic penetration depth or superfluid density depends on field in this way. The sublinear dependence of λ_{ab} on H is primarily due to the failure of Eq. (5) to account for all field-dependent contributions to the internal magnetic field distribution. In Refs. 28 and 34, the strong field dependence of λ_{ab} in $YBa_2Cu_3O_{6.95}$ determined by μSR was explained by the high anisotropy of the d-wave superconducting energy gap not accounted for in Eq. (5). A nonlocal supercurrent response to the applied field in the vicinity of the vortex cores stemming from the divergence of the coherence length at the gap nodes modifies the spatial distribution of field. With increasing H, the increased overlap of the regions around the vortex cores reduces the width of the μSR line shape. The gap anisotropy also results in a nonlinear supercurrent response to the applied field, resulting from a quasiclassical "Doppler shift" of the quasiparticle energy spectrum by the flow of superfluid around a vortex.[35] When the Doppler shift exceeds the energy gap, Cooper pairs are broken and λ_{ab} increases.

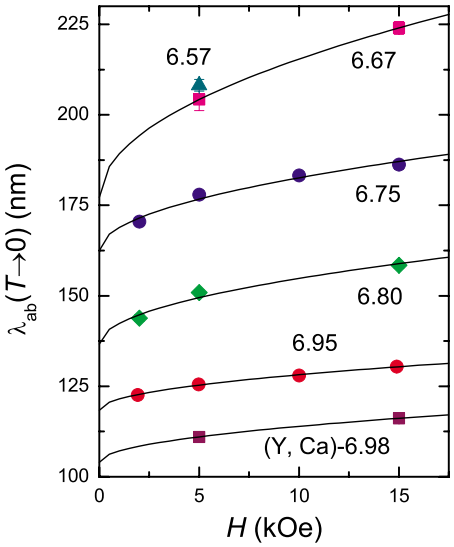

FIG. 6. (Color online) Magnetic field dependence of the extrapolated zero-temperature value of λ_{ab}. The solid curves are fits to $\lambda_{ab}(0,H)=\lambda_{ab}(0,0)+\beta\sqrt{H}$, where the coefficient β decreases with increasing hole doping.

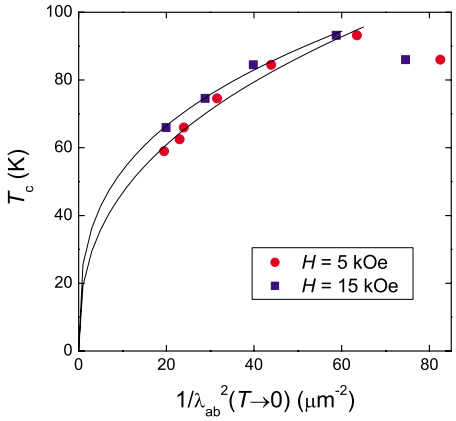

FIG. 7. (Color online) Dependence of T_c on $1/\lambda_{ab}^2(T\rightarrow 0)$. The two data points on the far right are for the overdoped sample $(Y,Ca)Ba_2Cu_3O_{6.98}$. The solid curves are fits to the data for $YBa_2Cu_3O_y$, yielding $T_c=(19.3\pm 1.7\ \mathrm{K}\ \mu\mathrm{m}^2)[1/\lambda_{ab}^2]^{0.38\pm 0.02}$ and $T_c=(25.5\pm 1.9\ \mathrm{K}\ \mu\mathrm{m}^2)[1/\lambda_{ab}^2]^{0.32\pm 0.02}$ at $H=5$ kOe and $H=15$ kOe, respectively.

These effects are not restricted to d-wave superconductors. Sizable nonlinear and/or nonlocal effects can also occur in s-wave superconductors with a smaller energy gap on one of the Fermi sheets and/or a highly anisotropic Fermi surface. Moreover, these anisotropies result in a rapid delocalization of quasiparticle core states with increasing H that modify $n(B)$. Indeed, strong field dependences of λ_{ab} from Eq. (5) have been observed in the multiband superconductor $NbSe_2$ (Ref. 15) and the marginal type-II superconductor V.[16] It has been experimentally established for a variety of materials,[15] including YBCO,[9] that the $H\rightarrow 0$ extrapolated value of λ_{ab} agrees with the magnetic penetration depth measured by other techniques in the Meissner phase. Consequently, we stress that only $\lambda_{ab}(H\rightarrow 0)$ can be considered a "true" measure of the magnetic penetration depth.

C. Hole-doping dependence

In Fig. 7, we show T_c as a function of $1/\lambda_{ab}^2(T\rightarrow 0)$ at two different fields. The more inclusive data set at $H=5$ kOe is described by $T_c\propto(1/\lambda_{ab}^2)^{0.38}$, which deviates substantially from the linear scaling in the Uemura plot. The power 0.38 is surprisingly close to 0.43 determined by Zuev *et al.* in a Meissner phase study of severely underdoped YBCO thin films.[10] It is surprising because these thin films have a superfluid density that is significantly lower than that of single crystals.[11] It is known from microwave studies of YBCO that

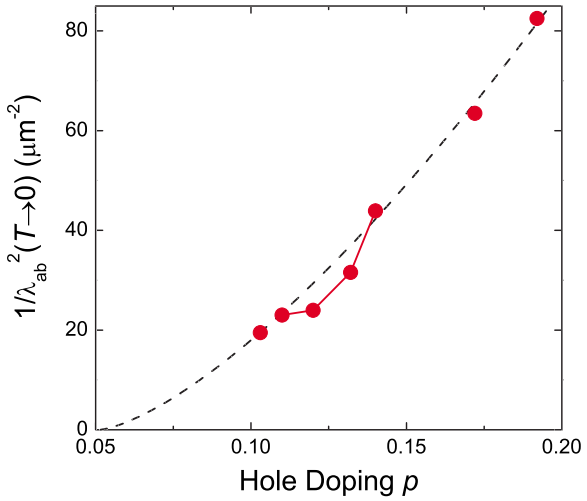

FIG. 8. (Color online) Dependence of $1/\lambda_{ab}^2(T\to 0)$ on hole-doping concentration p at $H=5$ kOe. The dashed curve is the function $1/\lambda_{ab}^2 \propto (p-0.05)^{1.42}$, where $p=0.5$ is the critical hole-doping concentration for the onset of superconductivity.

the doping dependences of λ_a and λ_b are not the same[9] due to the conductivity of the CuO chains.[36] Thus, there is no reason to expect the power ~ 0.4 to be universal for the cuprates. While a sublinear dependence of T_c on $1/\lambda_{ab}^2$ has also been inferred from more recent μSR measurements of the muon depolarization rate σ in other high-T_c superconductors,[37] the contributions of magnetism and FLL disorder to the μSR line shape were not factored out.

Figure 8 shows $1/\lambda_{ab}^2$ as a function of hole doping, where the values of p are determined from the dependence of T_c on p presented in Ref. 19 for similar YBCO single crystals. The behavior is consistent with other studies on cuprates indicating that the maximum value of $1/\lambda_{ab}^2$ is not reached before $p \approx 0.19$.[38,39] Our data are in the range $0.103 \leqslant p \leqslant 0.192$ and are described by $1/\lambda_{ab}^2 \propto (p-0.05)^{1.42}$, except near $p=0.125=\frac{1}{8}$.

The hole-doping dependences of $\sigma_{\rm dip}$ and $\sigma_{\rm FLL}$ at $H=5$ kOe are shown in Fig. 9(a). While $\sigma_{\rm dip}$ is independent of p, $\sigma_{\rm FLL}$ basically tracks $1/\lambda_{ab}^2$. Using the fitted values of $\sigma_{\rm FLL}$ and λ_{ab}, we have calculated the hole-doping dependence of the root-mean-square displacement $\langle s^2\rangle^{1/2}$ of the vortices from their positions in the perfect hexagonal FLL. As shown in Fig. 9(b), the degree of FLL disorder is small and as expected highest in the Ca-doped sample.

V. RESULTS FOR ξ_{ab}

A. Magnetic field dependence

The field dependences of ξ_{ab} are shown in Fig. 10. The increase in ξ_{ab} at low field, which corresponds to an expansion of the vortex cores, was previously reported for $YBa_2Cu_3O_{6.60}$ (Ref. 26) and $YBa_2Cu_3O_{6.95}$ (Refs. 27 and 28). In all samples, we find that ξ_{ab} scales as $1/\sqrt{H}$ over the field range explored here, which is proportional to the intervortex spacing.

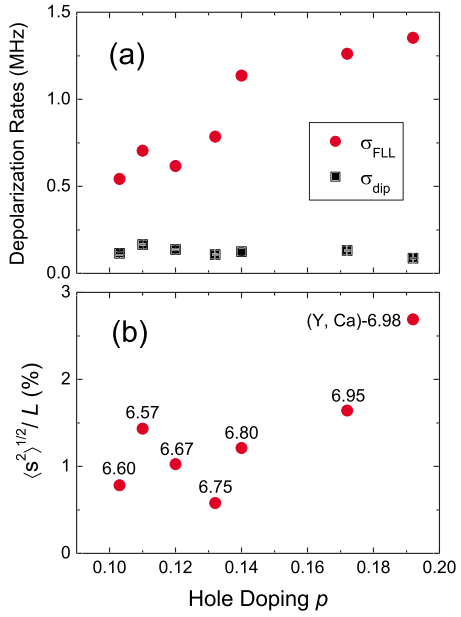

FIG. 9. (Color online) (a) Hole-doping dependences of the Gaussian depolarization rates $\sigma_{\rm FLL}$ and $\sigma_{\rm dip}$ at $T\to 0$ K and $H=5$ kOe. (b) Hole-doping dependence of the root-mean-square displacement $\langle s^2\rangle^{1/2}$ of the vortices from their positions in the perfect hexagonal FLL at $T\to 0$ K and $H=5$ kOe plotted as a percentage of the intervortex spacing L.

There have been two explanations put forth to explain a similar field dependence of the vortex core size in s-wave superconductors. Kogan and Zhelezina[40] have developed a model based on BCS theory that attributes the field dependence of the core size in clean high-κ s-wave superconductors to a field-dependent coherence length. However, theoretical calculations based on the microscopic equations without invoking a field-dependent coherence length show that the core size changes with field due to the intervortex transfer of quasiparticles.[41,42] A comparison of the field dependences of

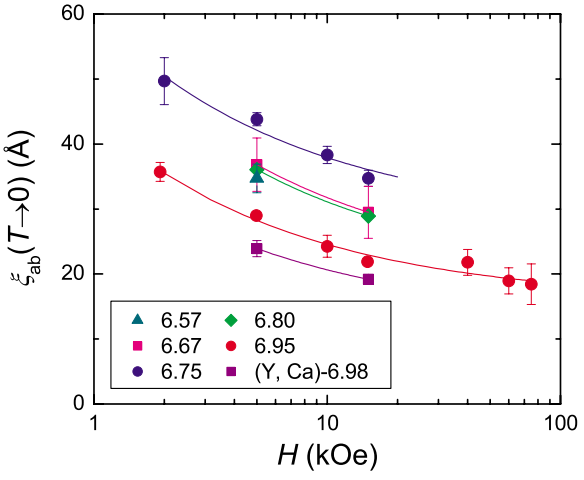

FIG. 10. (Color online) Magnetic field dependence of the extrapolated zero-temperature value of ξ_{ab}. The solid curves are fits to $\xi_{ab}(0,H)=a+b/\sqrt{H}$, where the coefficients a and b depend on the hole-doping concentration.

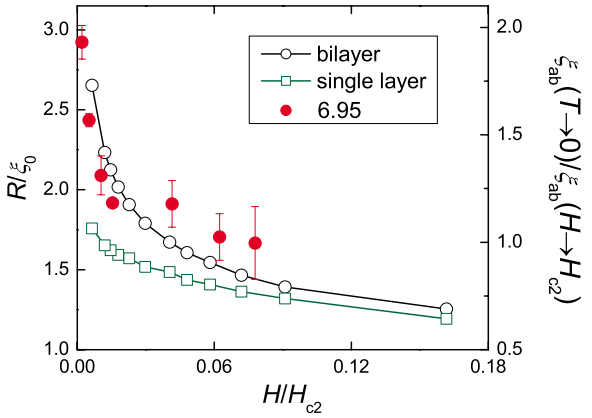

FIG. 11. (Color online) Calculated field-dependent core size R relative to the BCS coherence length ξ_0 for single-layer and bilayer models (see the Appendix). Also shown is the field dependence of $\xi_{ab}(T\to 0)$ in the $y=6.95$ sample normalized to the extrapolated value $\xi_{ab}(H\to H_{c2})=18.5$ Å and plotted as a function of H/H_{c2}, where $H_{c2}=\Phi_0/2\pi\xi_{ab}^2(H\to H_{c2})$. Note that here H_{c2} refers to the zero-temperature value $H_{c2}(0)$.

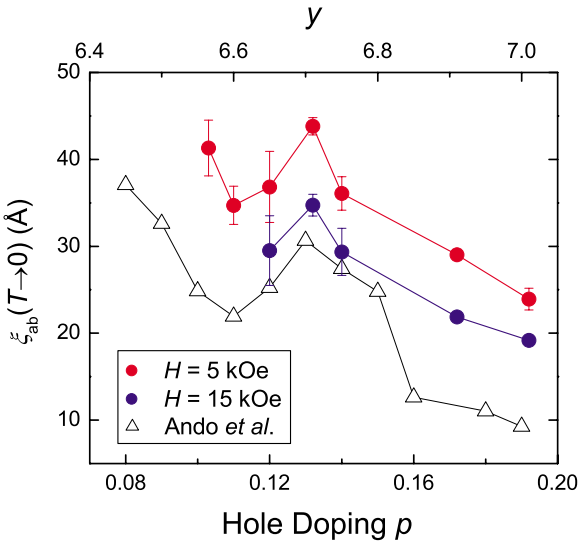

FIG. 12. (Color online) Hole-doping dependence of $\xi_{ab}(T\to 0)$ at $H=5$ kOe and $H=15$ kOe. Also shown are the data for ξ_{ab} from Ref. 44 plotted as a function of y, rather than p.

the core size measured by μSR and the electronic thermal conductivity in $NbSe_2$ (Ref. 15) and V_3Si (Ref. 14) strongly supports the latter picture. In YBCO, the low-energy quasiparticle core states should be extended along the nodal directions of the d-wave gap function.[43] This allows for a large transfer of low-energy quasiparticles between vortices at low field, which is further enhanced by an increase in vortex density. Hence, the vortex core size is predicted to shrink with increasing field.[41,42] However, the field dependence of ξ_{ab} in YBCO is considerably stronger than predicted for a pure d-wave superconductor. Consequently, we consider an alternative explanation.

In Fig. 11, we show that the field dependence of ξ_{ab}, in particular, the upturn at low field, can be explained by the presence of the CuO chains. The calculations of the core size R are based on a semiclassical Doppler-shift approximation (see the Appendix) for either a single-layer model representing a superconducting CuO_2 plane or a proximity-coupled model representing a CuO_2-CuO bilayer. In the bilayer model, there are two distinct energy scales for pair breaking: the energy gap associated with Cooper pairs in the CuO_2 planes and a smaller proximity-induced gap associated with the chains. It is the latter scale which is responsible for the expansion of the vortex cores at low field.

B. Hole-doping dependence

Figure 12 shows the hole-doping dependences of $\xi_{ab}(T\to 0)$ at $H=5$ kOe and $H=15$ kOe. Qualitatively, the doping dependence of ξ_{ab} is similar to that reported by Ando and Segawa from magnetoconductance measurements on detwinned YBCO single crystals.[44] The result of Ando and Segawa is also shown in Fig. 12, but plotted as ξ_{ab} versus y. Note that our data must be plotted as ξ_{ab} versus p because the hole concentration of our $y=6.60$ single crystals (grown in a crucible different from that used to grow the other samples) is smaller than that of $y=6.57$ (see Table I). The general trend of all data sets is an increase of ξ_{ab} with decreasing p. Such behavior has also been observed in the underdoped regime of $La_{2-x}Sr_xCuO_4$ (Refs. 45–47) and $Bi_2Sr_2CuO_{6+\delta}$.[48] With increasing magnetic field, our values for ξ_{ab} approach those determined by Ando and Segawa. Note that based on our proximity-induced model for the field dependence of ξ_{ab} (see the Appendix), it is the high-field values of ξ_{ab} that reflect the intrinsic superconductivity of the CuO_2 planes.

Since the doping dependences of ξ_{ab} at $H=5$ kOe and $H=15$ kOe in Fig. 12 are similar, we expect the hole-doping dependence of $H_{c2}^*\equiv\Phi_0/2\pi\xi_{ab}^2$ to qualitatively resemble that of the upper critical field H_{c2}. Figure 13 shows the hole-doping dependence of H_{c2}^* calculated from the values of ξ_{ab} at $H=5$ kOe. Consistent with the data of Ando and Segawa,

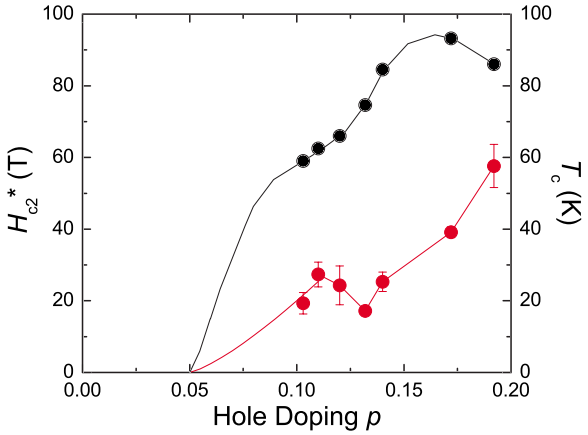

FIG. 13. (Color online) Plot of $H_{c2}^*=\Phi_0/2\pi\xi_{ab}^2(T\to 0)$ as a function of hole doping (red circles) using the values of $\xi_{ab}(T\to 0)$ at $H=5$ kOe. Also shown are the values of T_c (black circles). The black curve is the relation between T_c and p from Ref. 19.

H_{c2} decreases with decreasing p in the underdoped regime of YBCO and displays a dip near $\frac{1}{8}$ hole doping.

VI. SUMMARY AND CONCLUSIONS

We have simultaneously determined the hole-doping dependences of the magnetic penetration depth and the GL coherence length in the underdoped regime of YBCO. This was achieved by fitting μSR measurements in the vortex state to an analytical solution of the GL equations for the internal magnetic field distribution. In this type of analysis, the magnetic penetration depth is strictly defined as the $H \rightarrow 0$ extrapolated value of the fitted parameter λ_{ab}. The accuracy of this definition was established in previous studies of conventional superconductors.[15,16] Here, we have presented measurements showing a refinement of the Uemura plot for YBCO, where T_c is plotted as a function of the isolated quantity $1/\lambda_{ab}^2$ rather than the muon depolarization rate σ. We find that T_c exhibits a strong sublinear dependence on $1/\lambda_{ab}^2$, suggesting that T_c is not directly proportional to the superfluid density ρ_s. This result supports the same conclusion reached in several recent Meissner phase studies of YBCO.[9–11]

We have reported here a reduction of $1/\lambda_{ab}^2$ near $\frac{1}{8}$ hole-doping concentration. Suppression of $1/\lambda_{ab}^2$ or the muon depolarization rate σ near $\frac{1}{8}$ hole doping has only previously been observed in cuprates where p is controlled by cation substitution,[38,39] and was believed to indicate a tendency toward static stripe formation. Static stripes over the doping range investigated here were recently ruled out by inelastic neutron scattering experiments on YBCO.[49] We ourselves find no evidence for static spins in zero-field μSR or TF-μSR measurements on our samples.[22] However, the suppression of superconductivity near $p=\frac{1}{8}$ could be caused by fluctuating stripes, recently argued to be relevant in YBCO and other cuprates.[50] Experimental evidence for dynamic stripes in YBCO includes the detection of low-energy one-dimensional incommensurate modulations in $YBa_2Cu_3O_{6.50}$ by inelastic neutron scattering.[51]

Further evidence for suppression of superconductivity near $p=\frac{1}{8}$ is found in the hole-doping dependence of ξ_{ab}. In our measurements, ξ_{ab} is a parameter that characterizes the size of the vortex cores. While it mimics the behavior of the GL coherence length, ξ_{ab} is large at low field due to the contribution of the CuO chains to the spatial dependence of the superconducting order parameter. Enhancement of the GL coherence length or vortex core size near $\frac{1}{8}$ hole doping has also been observed in $La_{2-x}Sr_xCuO_4$.[45] Calculations by Mierzejewski and Maśka show that static or quasistatic stripes actually intensify H_{c2} by reducing diamagnetic pair breaking,[52] and hence cannot explain the growth of ξ_{ab} near $p=\frac{1}{8}$. On the other hand, Kadono *et al.* have shown that an expansion of the vortex cores with decreasing hole doping can result from a strengthening of antiferromagnetic correlations competing with superconductivity.[46] Thus, dynamic stripes are a viable explanation for the increased size of the vortex cores near $\frac{1}{8}$ hole doping.

ACKNOWLEDGMENTS

We gratefully acknowledge D. Broun, I. Vekhter, and A. J. Millis for helpful and informative discussions. We also thank Y. Ando for allowing us to reproduce his data here. This work was supported by the Canadian Institute for Advanced Research and the Natural Sciences and Engineering Research Council (NSERC) of Canada.

APPENDIX: SEMICLASSICAL CALCULATION OF THE VORTEX CORE SIZE

Calculations of the vortex core size are based on a generalization of the so-called "Doppler-shift" approximation for the vortex structure[53,54] to the case of YBCO, which is a multiband superconductor. In the case of YBCO, there is strong evidence that both the two-dimensional CuO_2 planes and one-dimensional CuO chains superconduct. Furthermore, it is likely that the chains are intrinsically normal, but are driven superconducting by the proximity effect. Proximity models for YBCO have been extensively described elsewhere.[36,55] The essential idea is that the superconductivity originates from a pairing interaction which is confined to the two-dimensional CuO_2 planes, and that the mixing of chain and plane wave functions induces superconductivity in the one-dimensional chain layers.

We adopt a simplified bilayer model consisting of a single plane and a single chain, with one Wannier orbital retained per unit cell for each layer. For comparison purposes, calculations are also performed for a single-layer model of an isolated superconducting plane. The Bogoliubov–de Gennes Hamiltonian for the bilayer is

$$\hat{H} = \sum_{ij} \hat{\Psi}_i^\dagger \begin{bmatrix} \tilde{t}_{1,ij} & \Delta_{ij} & t_\perp \delta_{i,j} & 0 \\ \Delta_{ij}^\dagger & -\tilde{t}_{1,ij}^* & 0 & -t_\perp \delta_{i,j} \\ t_\perp \delta_{i,j} & 0 & \tilde{t}_{2,ij} & 0 \\ 0 & -t_\perp \delta_{i,j} & 0 & -\tilde{t}_{2,ij}^* \end{bmatrix} \hat{\Psi}_j, \quad \text{(A1)}$$

where $\hat{\Psi}_i^\dagger = [\psi_{1i\uparrow}^\dagger \psi_{1i\downarrow} \psi_{2i\uparrow}^\dagger \psi_{2i\downarrow}]$ and $\psi_{ni\uparrow}^\dagger$ ($\psi_{ni\downarrow}$) are creation operators for quasiparticles (quasiholes) at lattice site i in layer n. Here, we take $n=1$ for the plane layer and $n=2$ for the chain layer. The parameters $\tilde{t}_{n,ij}$ and $t_\perp \delta_{i,j}$ are the single-electron hopping matrix elements between sites i and j within and between layers, respectively, while Δ_{ij} is the superconducting order parameter along bonds connecting nearest neighbor sites i and j. From the form of Eq. (A1), it is apparent that Δ_{ij} only couples quasiparticles belonging to the plane layer. The single-layer Hamiltonian is obtained by setting $t_\perp = 0$.

A magnetic field H applied perpendicular to the layers induces circulating currents in the superfluid. The superfluid velocity is given by $\mathbf{v_s} = \mathbf{M}^{-1} \cdot \mathbf{p_s}$, where $\mathbf{M}$ is the effective mass tensor, $\mathbf{p_s}(\mathbf{r}) = (2e\hbar/c)\mathbf{A}(\mathbf{r}) + \hbar \nabla \phi(\mathbf{r})$ is the superfluid momentum, $\mathbf{A}(\mathbf{r})$ is the magnetic vector potential, and $\phi(\mathbf{r})$ is the local phase of the order parameter. In the limit that $\phi(\mathbf{r})$ and $\mathbf{A}(\mathbf{r})$ are slowly varying functions, one can treat the superflow as uniform in the neighborhood of $\mathbf{r}$. Then, one can make a local gauge transformation[53,54] such that the

phase is removed from the order parameter and appears instead in the hopping matrix elements $\tilde{t}_{n,ij}$:

$$\tilde{t}_{n,ij} = t_{n,ij} e^{-i\mathbf{p_s}(\mathbf{r})\cdot(\mathbf{r}_i-\mathbf{r}_j)/2\hbar} \tag{A2a}$$

$$\approx t_{n,ij} + \frac{1}{2}\mathbf{v}_{ij}\cdot\mathbf{p_s}(\mathbf{r}), \tag{A2b}$$

where $t_{n,ij}$ are the hopping matrix elements in zero field and $\mathbf{v}_{ij}=-it_{n,ij}(\mathbf{r}_i-\mathbf{r}_j)/\hbar$ are the matrix elements of the zero-field quasiparticle velocity. Equation (A2b) follows from Eq. (A2a) in the limit that $\mathbf{p_s}$ is small. Then, the order parameter takes on the simple d-wave form $\Delta_{ij}=\frac{1}{2}\Delta(-1)^{y_i-y_j}$ which, in reciprocal space, corresponds to $\Delta_{\mathbf{k}}=\Delta[\cos(k_x a)-\cos(k_y a)]$, where a is the lattice constant. The local gauge transformation leads to a Doppler-shifted spectrum and is exact in the limit of slowly varying superfluid velocity. This procedure has been shown, in many circumstances, to provide a reasonable description of the vortex lattice.[53,54]

We take band structures which are appropriate for YBCO and adopt

$$t_{1,ij} = \begin{cases} t_0, & i=j \\ t_1, & i,j \text{ are nearest neighbors} \\ t_2, & i,j \text{ are next-nearest neighbors} \end{cases} \tag{A3}$$

and

$$t_{2,ij} = \begin{cases} t_3, & i=j \\ t_4, & i,j \text{ are nearest neighbors along } \hat{\mathbf{y}}. \end{cases} \tag{A4}$$

For this work, we measure energies in units of $|t_1|$ and take $\{t_0,\ldots,t_4\}=\{1,-1,0.45,2,-4\}$. In reciprocal space, the dispersions of the isolated plane and chain layers are then $\epsilon_{1\mathbf{k}}=t_0+2t_1[\cos(k_x a)+\cos(k_y a)]+4t_2\cos(k_x a)\cos(k_y a)$ and $\epsilon_{2\mathbf{k}}=t_3+2t_4\cos(k_y a)$, respectively. The chain-plane hopping matrix element $t_\perp$ is not well known in YBCO and is taken to be $t_\perp=0.75$.

For a slowly varying $\mathbf{p_s}(\mathbf{r})$, we can locally Fourier transform the Hamiltonian in the neighborhood of $\mathbf{r}$ to give

$$\hat{H}(\mathbf{r}) = \sum_k \hat{\Psi}_k^\dagger \begin{bmatrix} \epsilon_{1k}+\frac{1}{2}\mathbf{v}_{1k}\cdot\mathbf{p_s}(\mathbf{r}) & \Delta_k(\mathbf{r}) & t_\perp & 0 \\ \Delta_k(\mathbf{r}) & -\epsilon_{1k}+\frac{1}{2}\mathbf{v}_{1k}\cdot\mathbf{p_s}(\mathbf{r}) & 0 & -t_\perp \\ t_\perp & 0 & \epsilon_{2k}+\frac{1}{2}\mathbf{v}_{2k}\cdot\mathbf{p_s}(\mathbf{r}) & 0 \\ 0 & -t_\perp & 0 & -\epsilon_{2k}+\frac{1}{2}\mathbf{v}_{2k}\cdot\mathbf{p_s}(\mathbf{r}) \end{bmatrix} \hat{\Psi}_k, \tag{A5}$$

where $\mathbf{v}_{n\mathbf{k}}=\hbar^{-1}\partial\epsilon_{n\mathbf{k}}/\partial\mathbf{k}$ and $\hat{\Psi}_{\mathbf{k}}=N^{-1/2}\Sigma_i\hat{\Psi}_i$, where N is the number of k points in the sum in Eq. (A5).

We need to make an ansatz for $\mathbf{p_s}(\mathbf{r})$. For a single vortex in an isotropic medium, one has $\mathbf{p_s}(\mathbf{r})=(2\pi\hbar/r)\hat{\theta}$, where $\hat{\theta}$ is the azimuthal unit vector and the radius r is measured relative to the center of the vortex.[53] For the bilayer model, however, $\mathbf{p_s}(\mathbf{r})$ is not isotropic: the chains provide a conduction channel along the $\hat{\mathbf{y}}$ direction which is parallel to the isotropic plane conduction channel. We mimic this anisotropy by assuming that the superfluid momentum will be similar to that of a single-layer superconductor with an anisotropic (diagonal) effective mass tensor $\mathbf{M}$ with $M_{yy}<M_{xx}$. (For the single-layer model, we take $M_{xx}=M_{yy}$.) We then have two requirements which must be satisfied: $\nabla\times\mathbf{p_s}=2\pi\hbar\Sigma_{\mathbf{R}}\delta^2(\mathbf{r}-\mathbf{R})$ and $\nabla\cdot\mathbf{v_s}\equiv\nabla\cdot\mathbf{M}^{-1}\cdot\mathbf{p_s}=0$. The first requirement introduces vortex cores at the vortex lattice sites $\mathbf{R}$, while the latter incompressibility requirement is strictly true in regions where $\Delta(\mathbf{r})$ is uniform. This pair of equations is solved by

$$\mathbf{p_s}(\mathbf{r}) = \frac{2\pi\hbar}{L^2}\sum_{\mathbf{G}}{}' e^{i\mathbf{G}\cdot\mathbf{r}}\frac{i\mathbf{M}\cdot(\mathbf{G}\times\hat{\mathbf{z}})}{M_{xx}G_y^2+M_{yy}G_x^2}, \tag{A6}$$

where Σ' indicates that $\mathbf{G}=0$ is excluded from the sum, $\mathbf{G}$ are reciprocal lattice vectors of the magnetic unit cell (we assume a square lattice here) with area L^2 and magnetic length L. The results do not depend strongly on the ratio M_{yy}/M_{xx}, which we take to be 0.6 for the parameters chosen above. This choice minimizes $\nabla\cdot\mathbf{j}(\mathbf{r})$, where $\mathbf{j}(\mathbf{r})$ is the total (plane and chain) current in the bilayer,

$$\mathbf{j}(\mathbf{r}) = \frac{1}{N}\sum_{\mathbf{k}}\sum_{n=1}^{2}\langle\mathbf{v}_{1\mathbf{k}}+\mathbf{v}_{2\mathbf{k}}\rangle_{\mathbf{r}}, \tag{A7}$$

and $\langle\cdots\rangle_{\mathbf{r}}$ indicates the expectation value with respect to $\hat{H}(\mathbf{r})$ [Eq. (A5)]. In principle, one could improve on the approximation of Eq. (A6) by determining $\mathbf{p_s}(\mathbf{r})$ self-consistently from $\mathbf{j}(\mathbf{r})$; however, this will not change the qualitative physics of the vortex core expansion.

We then solve self-consistently for the order parameter

$$\Delta(\mathbf{r}) = -\frac{V}{N}\sum_{\mathbf{k}}[\cos(k_x a)-\cos(k_y a)]\langle\psi_{1-\mathbf{k}\downarrow}\psi_{1\mathbf{k}\uparrow}\rangle_{\mathbf{r}}, \tag{A8}$$

with $V=1.7$. Self-consistent solutions find that $\Delta(\mathbf{r})$ vanishes near the vortex core center and obtains an asymptotic value $\Delta_{\max}=0.35$ far from the vortex core. In order to measure the vortex core size, we define a quantity $\delta\Delta(\mathbf{r})=\Delta_{\max}-\Delta(\mathbf{r})$. The vortex core size is then defined by the first moment of the radial coordinate r with respect to $\delta\Delta(\mathbf{r})$:

$$R = \frac{\sum_{\mathbf{r}} r\,\delta\Delta(\mathbf{r})}{\sum_{\mathbf{r}} \delta\Delta(\mathbf{r})}, \tag{A9}$$

where $r=0$ corresponds to the vortex core center. For presentation purposes, R is shown relative to the BCS coherence length $\xi_0 \equiv \hbar v_F / \pi\Delta_{\max}$, where v_F is the average of the Fermi velocity on the Fermi surface. The magnetic field is related to the magnetic length by $H=\Phi_0/L^2$, where Φ_0 is the superconducting flux quantum. For presentation purposes, H is scaled by the upper critical field, $H_{c2} \equiv \Phi_0/2\pi\xi_0^2$, so that $H/H_{c2}=2\pi\xi_0^2/L^2$.

[1] D. R. Harshman *et al.*, Phys. Rev. B **36**, 2386 (1987).
[2] Y. J. Uemura *et al.*, Phys. Rev. B **38**, 909 (1988).
[3] D. R. Harshman, L. F. Schneemeyer, J. V. Waszczak, G. Aeppli, R. J. Cava, B. Batlogg, L. W. Rupp, E. J. Ansaldo, and D. Ll. Williams, Phys. Rev. B **39**, 851 (1989).
[4] B. Pümpin *et al.*, Phys. Rev. B **42**, 8019 (1990).
[5] Y. J. Uemura *et al.*, Phys. Rev. Lett. **62**, 2317 (1989).
[6] Y. J. Uemura *et al.*, Phys. Rev. Lett. **66**, 2665 (1991).
[7] W. N. Hardy, D. A. Bonn, D. C. Morgan, R. Liang, and K. Zhang, Phys. Rev. Lett. **70**, 3999 (1993).
[8] J. E. Sonier *et al.*, Phys. Rev. Lett. **72**, 744 (1994).
[9] T. Pereg-Barnea, P. J. Turner, R. Harris, G. K. Mullins, J. S. Bobowski, M. Raudsepp, R. Liang, D. A. Bonn, and W. N. Hardy, Phys. Rev. B **69**, 184513 (2004).
[10] Y. Zuev, M. S. Kim, and T. R. Lemberger, Phys. Rev. Lett. **95**, 137002 (2005).
[11] D. M. Broun, P. J. Turner, W. A. Huttema, S. Ozcan, B. Morgan, R. Liang, W. N. Hardy, and D. A. Bonn, arXiv:cond-mat/0509223 (unpublished).
[12] A. Rüfenacht, J.-P. Locquet, J. Fompeyrine, D. Caimi, and P. Martinoli, Phys. Rev. Lett. **96**, 227002 (2006).
[13] J. E. Sonier, J. H. Brewer, and R. F. Kiefl, Rev. Mod. Phys. **72**, 769 (2000).
[14] J. E. Sonier, F. D. Callaghan, R. I. Miller, E. Boaknin, L. Taillefer, R. F. Kiefl, J. H. Brewer, K. F. Poon, and J. D. Brewer, Phys. Rev. Lett. **93**, 017002 (2004).
[15] F. D. Callaghan, M. Laulajainen, C. V. Kaiser, and J. E. Sonier, Phys. Rev. Lett. **95**, 197001 (2005).
[16] M. Laulajainen, F. D. Callaghan, C. V. Kaiser, and J. E. Sonier, Phys. Rev. B **74**, 054511 (2006).
[17] R. Liang, D. A. Bonn, and W. N. Hardy, Physica C **304**, 105 (1998).
[18] R. Liang, P. Dosanjh, D. A. Bonn, D. J. Baar, J. F. Carolan, and W. N. Hardy, Physica C **195**, 51 (1992).
[19] R. Liang, D. A. Bonn, and W. N. Hardy, Phys. Rev. B **73**, 180505(R) (2006).
[20] A. Yaouanc, P. Dalmas de Réotier, and E. H. Brandt, Phys. Rev. B **55**, 11107 (1997).
[21] S. P. Brown, D. Charalambous, E. C. Jones, E. M. Forgan, P. G. Kealey, A. Erb, and J. Kohlbrecher, Phys. Rev. Lett. **92**, 067004 (2004).
[22] J. E. Sonier *et al.*, Phys. Rev. B **76**, 064522 (2007).
[23] D. Dulić, S. J. Hak, D. van der Marel, W. N. Hardy, A. E. Koshelev, R. Liang, D. A. Bonn, and B. A. Willemsen, Phys. Rev. Lett. **86**, 4660 (2001).
[24] E. H. Brandt, J. Low Temp. Phys. **73**, 355 (1988).
[25] A. Schenck, *Muon Spin Rotation Spectroscopy: Principles and Applications in Solid State Physics* (Adam Hilger, Bristol, England, 1985).
[26] J. E. Sonier *et al.*, Phys. Rev. Lett. **79**, 2875 (1997).
[27] J. E. Sonier, R. F. Kiefl, J. H. Brewer, D. A. Bonn, S. R. Dunsiger, W. N. Hardy, R. Liang, R. I. Miller, D. R. Noakes, and C. E. Stronach, Phys. Rev. B **59**, R729 (1999).
[28] J. E. Sonier, J. H. Brewer, R. F. Kiefl, G. D. Morris, R. I. Miller, D. A. Bonn, J. Chakhalian, R. H. Heffner, W. N. Hardy, and R. Liang, Phys. Rev. Lett. **83**, 4156 (1999).
[29] D. R. Harshman, W. J. Kossler, X. Wan, A. T. Fiory, A. J. Greer, D. R. Noakes, C. E. Stronach, E. Koster, and J. D. Dow, Phys. Rev. B **69**, 174505 (2004).
[30] J. E. Sonier, D. A. Bonn, J. H. Brewer, W. N. Hardy, R. F. Kiefl, and R. Liang, Phys. Rev. B **72**, 146501 (2005).
[31] R. Khasanov, A. Shengelaya, A. Maisuradze, F. La Mattina, A. Bussmann-Holder, H. Keller, and K. A. Müller, Phys. Rev. Lett. **98**, 057007 (2007).
[32] L. B. Ioffe and A. J. Millis, J. Phys. Chem. Solids **63**, 2259 (2002).
[33] M. Sutherland *et al.*, Phys. Rev. B **67**, 174520 (2003).
[34] M. H. S. Amin, I. Affleck, and M. Franz, Phys. Rev. B **58**, 5848 (1998).
[35] G. E. Volovik, JETP Lett. **58**, 469 (1993).
[36] W. A. Atkinson and J. P. Carbotte, Phys. Rev. B **52**, 10601 (1995).
[37] J. L. Tallon, J. W. Loram, J. R. Cooper, C. Panagopoulos, and C. Bernhard, Phys. Rev. B **68**, 180501(R) (2003).
[38] C. Bernhard, J. L. Tallon, Th. Blasius, A. Golnik, and Ch. Niedermayer, Phys. Rev. Lett. **86**, 1614 (2001).
[39] C. Panagopoulos, J. L. Tallon, B. D. Rainford, T. Xiang, J. R. Cooper, and C. A. Scott, Phys. Rev. B **66**, 064501 (2002).
[40] V. G. Kogan and N. V. Zhelezina, Phys. Rev. B **71**, 134505 (2005).
[41] M. Ichioka, A. Hasegawa, and K. Machida, Phys. Rev. B **59**, 184 (1999).
[42] M. Ichioka, A. Hasegawa, and K. Machida, Phys. Rev. B **59**, 8902 (1999).
[43] M. Ichioka, N. Hayashi, N. Enomoto, and K. Machida, Phys. Rev. B **53**, 15316 (1996).
[44] Y. Ando and K. Segawa, Phys. Rev. Lett. **88**, 167005 (2002).
[45] H. H. Wen, H. P. Yang, S. L. Li, X. H. Zeng, A. A. Soukiassian, W. D. Si, and X. X. Xi, Europhys. Lett. **64**, 790 (2003).
[46] R. Kadono *et al.*, Phys. Rev. B **69**, 104523 (2004).
[47] Y. Wang, L. Li, and N. P. Ong, Phys. Rev. B **73**, 024510 (2006).
[48] F. Bouquet, L. Fruchter, I. Sfar, Z. Z. Li, and H. Raffy, Phys. Rev. B **74**, 064513 (2006).
[49] V. Hinkov, S. Pailhés, P. Bourges, Y. Sidis, A. Ivanov, A. Kulakov, C. T. Lin, D. P. Chen, C. Bernhard, and B. Keimer, Nature (London) **430**, 650 (2004).
[50] M. Vojta, T. Vojta, and R. K. Kaul, Phys. Rev. Lett. **97**, 097001 (2006).

[51] C. Stock, W. J. L. Buyers, R. Liang, D. Peets, Z. Tun, D. Bonn, W. N. Hardy, and R. J. Birgeneau, Phys. Rev. B **69**, 014502 (2004).

[52] M. Mierzejewski and M. M. Maśka, Phys. Rev. B **66**, 214527 (2002).

[53] I. Vekhter, P. J. Hirschfeld, and E. J. Nicol, Phys. Rev. B **64**, 064513 (2001).

[54] D. Knapp, C. Kallin, and A. J. Berlinsky, Phys. Rev. B **64**, 014502 (2001).

[55] W. A. Atkinson, Phys. Rev. B **59**, 3377 (1999).